

## Predicting non-deposition sediment transport in sewer pipes using Random forest

Montes, Carlos; Kapelan, Zoran; Saldarriaga, Juan

**DOI**

[10.1016/j.watres.2020.116639](https://doi.org/10.1016/j.watres.2020.116639)

**Publication date**

2021

**Document Version**

Accepted author manuscript

**Published in**

Water Research

**Citation (APA)**

Montes, C., Kapelan, Z., & Saldarriaga, J. (2021). Predicting non-deposition sediment transport in sewer pipes using Random forest. *Water Research*, 189, 1-11. Article 116639.  
<https://doi.org/10.1016/j.watres.2020.116639>

**Important note**

To cite this publication, please use the final published version (if applicable).  
Please check the document version above.

**Copyright**

Other than for strictly personal use, it is not permitted to download, forward or distribute the text or part of it, without the consent of the author(s) and/or copyright holder(s), unless the work is under an open content license such as Creative Commons.

**Takedown policy**

Please contact us and provide details if you believe this document breaches copyrights.  
We will remove access to the work immediately and investigate your claim.

1 **Predicting non-deposition sediment transport in sewer pipes using**  
2 **Random Forest**

3 Carlos Montes<sup>a\*</sup>, Zoran Kapelan<sup>b</sup> and Juan Saldarriaga<sup>c</sup>

4 *<sup>a</sup>Department of Civil and Environmental Engineering, Universidad de los Andes, Bogotá,*  
5 *Colombia; e-mail: cd.montes1256@uniandes.edu.co*

6 *<sup>b</sup>Department of Water Management, Delft University of Technology, Delft, Netherlands;*  
7 *e-mail: Z.Kapelan@tudelft.nl*

8 *<sup>c</sup>Department of Civil and Environmental Engineering, Universidad de los Andes, Bogotá,*  
9 *Colombia; e-mail: jsaldarr@uniandes.edu.co*

10 \*corresponding author; Correspondence address: Cra 1 Este No. 19A – 40 Bogota  
11 (Colombia); Tel.: +57-1-339-49-49 (ext. 1765)

# **Predicting non-deposition sediment transport in sewer pipes using Random Forest**

## **Abstract**

Sediment transport in sewers has been extensively studied in the past. This paper aims to propose a new method for predicting the self-cleansing velocity required to avoid permanent deposition of material in sewer pipes. The new Random Forest (RF) based model was implemented using experimental data collected from the literature. The accuracy of the developed model was evaluated and compared with ten promising literature models using multiple observed datasets. The results obtained demonstrate that the RF model is able to make predictions with high accuracy for the whole dataset used. These predictions clearly outperform predictions made by other models, especially for the case of non-deposition with deposited bed criterion that is used for designing large sewer pipes. The volumetric sediment concentration was identified as the most important parameter for predicting self-cleansing velocity.

Keywords: non-deposition; random forest; sediment transport; self-cleansing; sewer systems.

## **1. INTRODUCTION**

Designing sediment-carrying sewer systems is a well-known field of research in hydraulic engineering. This interest is explained by the problems related to the presence of material in the systems. Due to the varying environmental conditions (i.e. loading and sediment characteristics and intermittent flow), the risk of building up a permanent sediment deposit increases during dry weather seasons. These deposits lead to problems such as reduced pipe capacity, increased roughness, and premature overflows. As an example, Ackers et al. (2001) showed that the presence of a permanent deposit at the bottom of sewer pipes increases hydraulic roughness and reduces discharge capacity by about 20%.

The most common criterion to avoid permanent deposit of material in sewer pipes is known as non-deposition. Several authors (Safari et al., 2018; Vongvisessomjai et al., 2010) have classified this criterion into two subgroups: 1) Non-deposition without deposited bed and 2) Non-deposition with deposited bed. Both groups are based on the presence of sediments at the bottom of the pipe. In the first case, high water velocities produce an individual and separate movement of the particles by slicing or rolling over the pipe invert, i.e. without deposited bed. In contrast, the second case is seen when lower water velocities are presented and the particles are grouped and move as a transitional deposited bed.

In the case of ‘without deposited bed’, traditional criteria of minimum velocities and shear stress values are commonly found in water utilities standards and industry design codes. Generally, these standards and codes suggest values ranging from 0.30 m s<sup>-1</sup> to 1.0 m s<sup>-1</sup> for minimum velocity and from 1.0 Pa to 4.0 Pa for shear stress (Montes et al., 2019; Nalluri and Ab Ghani, 1996; Vongvisessomjai et al., 2010). Several authors (Merritt and Enfinger, 2019; Nalluri and Ab Ghani, 1996) have shown how traditional threshold values lead to over-design of small diameter pipes and under-design of large diameter pipes (as a rule-of-thumb, pipes with diameter greater than 500 mm). Consequently, large sewers commonly require frequent removal of sediment deposits (Ackers et al., 2001) because of the minimum self-cleansing value adopted during the design stage. A unique design value is inadequate; hence sediment characteristics and hydraulic conditions must be included in the definition of the self-cleansing design criterion.

According to Safari and Aksoy (2020), existing traditional self-cleansing criteria can be up to 20% different from laboratory-scale measured values. The channel cross-section is relevant in the choice of the self-cleansing criterion. For example, rectangular

cross-sections require lower velocities compared to V-bottom or U-shape channels. Even criteria based on the Shields diagram, such as the Camp criterion, seem to be inadequate to define the self-cleansing value due to the non-inclusion of sediment concentration.

The above has motivated extensive experimental research (Ab Ghani, 1993; El-Zaemey, 1991; May, 1993; May et al., 1989; Mayerle, 1988; Montes et al., 2020a, 2020b; Ota, 1999; Perrusquía, 1991; Vongvisessomjai et al., 2010) aiming to collect data and developing models for predicting the self-cleansing velocity as a function of sediment characteristics and system hydraulics, based on the concept of non-deposition. These studies have been carried out at laboratory scale under well-controlled and steady flow conditions, using non-cohesive sediments. Different authors collected data in pipes with different materials (e.g. concrete, acrylic or PVC, among other materials) and internal diameters, ranging from 100 mm to 595 mm. In the end, all these studies proposed a model for predicting the self-cleansing conditions in practice that was either developed with their own experimental data or using the benchmark data reported in the literature. Most models developed are regression-based and include the group of input parameters that most affect the prediction of the self-cleansing velocity (Ackers et al., 2001; Ebtehaj and Bonakdari, 2016a; May et al., 1996). Most of these models are in the form of:

$$\frac{V_l}{\sqrt{gd(S_s - 1)}} = aC_v^b \left( \frac{d}{R} \text{ or } \frac{d}{D} \right)^c \lambda^e D_{gr}^f \left( \frac{W_b}{Y} \text{ or } \frac{y_s}{Y} \text{ or } \frac{y_s}{D} \right)^g \left( \frac{P}{B} \right)^h \quad (1)$$

where  $V_l$  is the self-cleansing velocity,  $d$  the mean particle diameter,  $g$  the gravity acceleration coefficient,  $S_s$  the specific gravity of sediments,  $C_v$  the volumetric sediment concentration,  $R$  the hydraulic radius,  $D$  the pipe diameter,  $\lambda$  the channel friction factor,  $D_{gr}$  the dimensionless grain size  $\left( = \left( \frac{(S_s - 1)gd^3}{\nu^2} \right)^{\frac{1}{3}} \right)$ ,  $\nu$  the water kinematic viscosity,  $W_b$  the sediment deposited width,  $P$  the wetted perimeter,  $y_s$  the sediment deposited thickness,  $B$  the water surface width,  $Y$  the water level and  $a, b, c, e, f, g$  and  $h$  regression

coefficients. Other parameters as  $V_t$  the threshold velocity required to initiate movement  
 $\left(= 0.125(gd(S_s - 1))^{0.5}(Y/d)^{0.47}\right)$  and  $S_o$  the pipe slope have also been included in  
regression models (May et al., 1996; Montes et al., 2020a).

Most of above studies for both non-deposition criteria, have developed predictive  
models which tend to be overfitted to their own experimental data. This problem can be  
seen especially in the earlier works, where no advanced techniques were used to develop  
regression models. For example, several authors (Montes et al., 2020b; Safari et al., 2018)  
have pointed out that early work of Mayerle's (1988) has developed a model that shows  
high accuracy prediction with its data and poor prediction when other datasets are used.  
In contrast, recent regression-models, which used novel techniques such as Evolutionary  
Polynomial Regression – Multi-Objective Genetic Algorithm (EPR-MOGA) and Least  
Absolute Shrinkage and Selection Operator (LASSO) have demonstrated better  
prediction results (Montes et al., 2020a, 2020b).

In order to address the above overfitting issue in regression models, new Machine  
Learning (ML) and Artificial Intelligence (AI) techniques have been introduced for  
predicting the self-cleansing velocity based on the concept of non-deposition sediment  
transport. Examples of models developed for the 'without deposited bed' case include  
using techniques such as Artificial Neural Network (ANN) (Ebtehaj and Bonakdari,  
2013), Support Vector Regression (SVR) coupled with the Firefly Algorithm (Ebtehaj  
and Bonakdari, 2016b), the Group Method of Data Handling (GMDH) (Ebtehaj and  
Bonakdari, 2016a), neuro-fuzzy inference system combined with the Particle Swarm  
Optimisation (ANFIS-PSO) (Ebtehaj et al., 2019), Decision Trees (DT), Generalised  
Regression Neural Network (GRNN), Multivariate Adaptive Regression Splines (MARS)  
(Safari, 2019) and Extreme Learning Machine (ELM) (Ebtehaj et al., 2020). For the other  
case of 'non-deposition with deposited bed', fewer ML/AI type models have been

developed. Examples include models based on Particle Swarm Optimisation (PSO) algorithm (Safari et al., 2017), Gene Expression Programming (GEP) (Roushangar and Ghasempour, 2017) and Multigene Genetic Programming (MGP) (Safari and Danandeh Mehr, 2018).

The above models, developed using different ML/AI techniques (for both non-deposition criteria), have improved the prediction accuracy of self-cleansing velocities and addressed the issues of model overfitting but only partially. As noted by Zendehboudi et al. (2018), these models still tend to have rather limited extrapolation capabilities meaning that once they are applied to datasets that were not used for their training they tend to underperform. Also, the ML/AI based models developed so far are largely black-box type models (e.g. ANN) meaning that, unlike white-box type regression models, they suffer from low interpretability of physical significance of model inputs (i.e. explanatory factors), and interactions with the model output.

The aim of this paper is to overcome above deficiencies using the Random Forest (RF) technique for predicting self-cleansing sewer velocities. RF (Breiman, 2001) is a flexible and interpretable supervised ML technique that combines the results (outputs) of multiple individual decision trees to make a prediction of interest. Due to its good characteristics and easy application, it has been widely used for addressing many other problems in water engineering. Tyrallis et al. (2019) showed a full review of studies in which RF was successfully applied to water resources problems.

Using the RF technique, a new predictive self-cleansing model is developed and presented here for both non-deposition criteria (with and without deposited bed). This model aims to increase prediction accuracy whilst avoiding overfitting issues and enabling interpretability of results obtained. The new modelling technique is compared to ten literature models using multiple datasets.

## 2. DATA

### 2.1. *Non-deposition without deposited bed data*

Several experimental data were collected from the literature to implement the RF method. Mayerle (1988) studied the sediment transport in a 152 mm diameter pipe and in two rectangular channels of 311.5 mm and 462.3 mm bottom width ( $W$ ) using granular sands ranging from 0.50 mm to 8.74 mm. Ab Ghani (1993) collected 221 data in 154 mm, 305 mm and 450 mm diameter pipes, testing sands between 0.46 mm and 8.40 mm. Ota (1999) used a 225 mm concrete pipe with a constant slope of 0.002, varying the volumetric sediment concentration between 4.2 ppm to 59.4 ppm. Vongvisessomjai et al. (2010) used two circular PVC pipes of 100 mm and 150 mm diameter to study the bedload and suspended load transport. Montes et al. (2020a) collected experimental data in a 242 mm acrylic pipe using granular material with a mean particle diameter of 0.35 mm and 1.51 mm. Montes et al. (2020b) carried out 107 experiments in a 595 mm PVC pipe, using sediments ranging from 0.35 mm to 2.6 mm.

### 2.2. *Non-deposition with deposited bed data*

For the non-deposition with deposited bed, El-Zaemey (1991) studied the sediment transport in a 305 mm diameter pipe, using granular particles ranging from 0.53 mm to 8.40 mm. Perrusquía (1991) carried out experiments in a 225 mm diameter pipe, varying the sediment concentration from 18.7 ppm to 408.0 ppm. Ab Ghani (1993) collected the deposited bed data only in the 450 mm concrete pipe and using granular sand with a mean particle diameter of 0.72 mm. May (1993) extended their previous study (May et al., 1989) and collected experimental data with sediment thickness varying from 57.6 mm to 129.6 mm. Finally, Montes et al. (2020b) carried out experiments in a 595 mm PVC pipe, considering a relative sediment thickness ( $y_s/D$ ) between 0.13% and



1.11%. Table 1 outlines the characteristics of the data used for developing the RF algorithm.

[Table 1 near here]

As shown in Table 1, a total of 664 and 454 data are available for the development of models without deposited bed and the deposited bed criteria, respectively.

### 3. MEHODOLOGY

#### 3.1. *Random Forest Model*

Random Forest model developed here predicts the particle Froude number ( $F_r^*$ ) as a function of several well-known dimensionless explanatory factors (Kargar et al., 2019; Vongvisessomjai et al., 2010):

$$F_r^* = \frac{V_l}{\sqrt{gd(S_s - 1)}} = f\left(C_v, D_{gr}, \frac{d}{R}, \lambda, \frac{y_s}{D}\right) \quad (2)$$

Random forest (RF) is a bagging algorithm for regression and classification problem proposed by Breiman (2001). This is a low-variance method, which randomly split the training data and the input variables predictors to build a set of  $b$  decision trees ( $B_t$ ). The results of all decision trees generated from bootstrapped training samples ( $T_b(x; \theta_b)$ ) are then averaged, i.e. the final result ( $\hat{y}(x)$ ) is the average of the output of all decision trees (as shown in Eq. (3)). This procedure ensures the reduction of the model variance and consequently, the reduction of the risk of overfitting. A simplified conceptual diagram of the RF method is shown in Figure 1.

$$\hat{y}(x) = \frac{1}{B_t} \sum_{b=1}^{B_t} T(x; \theta_b) \quad (3)$$

[Figure 1 near here]

In this paper, the R package ‘RandomForest’ (Liaw and Wiener, 2002) was used for constructing both non-deposition, without deposited bed and deposited bed, self-cleansing models. The number of predictors considered at each split ( $mtry$ ) and the number of trees in the forest ( $B_t$ ) are the parameters that define the structure of the RF regression model. The  $mtry$  parameter is estimated by using the `rfcv()` function, which shows the cross-validation performance for each number of predictors. In addition, the optimal number of trees is defined as the value that minimises the Mean Square Error (MSE) value of the training data. These parameters are estimated and the results are shown in Figure 2. According to this figure, the optimal number of features (i.e. the random predictors used in each tree) are three and four non-dimensional parameters for the cases of without deposited bed and with deposited bed, respectively. Similarly, the optimal number of trees is 471 for without deposited bed and 229 for with deposited bed.

**[Figure 2 near here]**

Cross-validation is carried out during the training stage using out-of-bag (OOB) samples. As mentioned above, the method randomly bootstraps the training sample, that is, some of the training data are left out to build each decision tree. Only two out of three parts of the total training data are used to build the tree (Breiman, 2001). Based on this, data not included in the bootstrapped sample (OOB data) are predicted, and the prediction error is averaged over the trees that do not include these data (OOB Error).

### **3.1.1. *Splitting of training and testing data***

The whole benchmarking data collected from the literature are used for both training and testing stages of the RF model. Usually, 75% of the data is used during the training stage of the model and the other 25% to validate the results. According to Safari (2020), the range of variation in the training data has direct implications for model performance (i.e. accuracy). As a result, the model can show overfitting issues and poor extrapolation

capabilities when narrow datasets are used in the training stage (i.e. data with a low range of variation).

Checking the non-overfitting of the RF model is carried out by using several sizes in the training and testing data (i.e. changing the percentage of data used as training and testing) and by verifying the error, defined by the Coefficient of Determination ( $R^2$ ) (as shown in Eq. (14)). For this, ten different combinations of percentages are defined (i.e. % of the training data : % of the testing data = [5:95, 15:85, 25:75, 35:65, 45:55, 55:45, 65:35, 75:25, 85:15, 95:5]), randomly changing the ranges of the training and testing data, and developing 100 RF models for each combination. As a result, 1000 RF models are trained and the error is estimated for both training and testing stage. Using this information, several boxplots are constructed showing the  $R^2$  variation for each stage. Figure 3 shows how the model error decreases as the training sample size increases. For example, when only 5% of the whole dataset is used for training the model and the remaining 95% for testing it, the error varies between 0.84 and 0.96, for the training stage, and between 0.39 and 0.73 for the testing stage. This clearly shows that the model is under-trained; however, when the ratio is greater than 50:50 the error tends to be constant and slightly variable for both stages. Ratios greater than 90:10 tend to generate unsatisfactory results for the testing stage, i.e. the model is over-trained and shows high variation in the error, i.e. overfitting, (as shown in Figure 3b). Based on this, a combination of 75:25 is taken as optimal for implementing the model.

**[Figure 3 near here]**

The variation of the data used for training and testing dataset is presented in Table 2.

**[Table 2 near here]**

Using the above considerations, the RF model is implemented with the optimal parameters defined in Figure 2 and using the ranges of variation of the training data outlined in Table 2. The full data collected from the literature are shown in the Supplementary material. Table S1 and Table S2 show the data for non-deposition without and with deposited bed, respectively, and the corresponding RF particle Froude number predictions. The implemented code for the RF method is shown in Figure 4. An example of one of the 471 decision trees generated by the RF model, for the non-deposition without deposited bed, is shown in Figure S1, in the Supplementary material.

**[Figure 4 near here]**

### 3.1.2. *Measure of feature importance*

Note that in this paper, a decrease in model accuracy when the  $j$ th variable is permuted (i.e. the percentage of the increase in the MSE,  $\%IncMSE$ ) is considered as a measure of the importance of a model input variable. This index shows the strength of each explanatory variable based on the reduction of the MSE. The step-by-step to calculate the  $\%IncMSE$  is shown as follows (Hastie et al., 2009):

- (1) Calculate the MSE of the OOB-sample data in each tree of the forest ( $MSE_b$ ).
- (2) Randomly permute the value of the  $j$ th explanatory variable and calculate the MSE ( $MSE_j$ ).
- (3) Finally, calculate  $\%IncMSE$  for each explanatory variable as:

$$\%IncMSE = 100 \cdot \frac{MSE_j - MSE_b}{MSE_b} \quad (4)$$

As a result, the more the  $\%IncMSE$  increases for a variable, the more important it is.

## 3.2. Performance Assessment

### 3.2.1. Models used for comparing the RF results

In order to evaluate the RF model performance, it is compared to several literature models. The models selected for comparison are the replicable white-box models with high prediction accuracy reported in the literature and two black-box models where the implementing code is provided in the original papers. Other black-box models cannot be evaluated due to the limited replicability shown by these models (e.g. ANN). Based on this, in the case of non-deposition without deposited bed, seven models selected are the EPR-MOGA model (Montes et al., 2020a), the GEP model (Kargar et al., 2019), the MARS model (Safari, 2019), the May et al. (1996) model, the Safari and Aksoy (2020) model, the ANFIS-PSO model (Ebtehaj et al., 2019) and the ELM model (Ebtehaj et al., 2020). In the case of non-deposition with deposited bed, three models used for comparison are the PSO model (Safari and Shirzad, 2019), the LASSO model (Montes et al., 2020b) and the MGP model (Safari and Danandeh Mehr, 2018). The EPR-MOGA, LASSO, May et al. (1996) and Safari and Aksoy (2020) are the regression type models whilst GEP, MARS, ANFIS-PSO, ELM, PSO and MGP models make use of ML/AI techniques.

The equations used by above ten models are as follows:

EPR-MOGA:

$$\frac{V_l}{\sqrt{gd(S_s - 1)}} = 5.6C_v^{0.16} \left(\frac{d}{R}\right)^{-0.58} S_o^{0.14} D_{gr}^{0.02} \quad (5)$$

GEP:

$$\begin{aligned} \frac{V_l}{\sqrt{gd(S_s - 1)}} = & \frac{3.05C_v^{0.16}}{\operatorname{atan}\left(\operatorname{atan}\left(\sqrt{\frac{d}{R}}\right)\right)} + \operatorname{atan}(3.41 - \ln(D_{gr})) \\ & + \operatorname{atan}\left(\tan\left(\left(8.37 - 7.99\lambda + \frac{d}{R}\lambda\right)^2\right)\right) + \ln\left(\left(\left(\frac{d}{R}\right)^3\right)^{2\lambda}\right) \end{aligned} \quad (6)$$

269 MARS:

$$\begin{aligned} \frac{V_l}{\sqrt{gd(S_s - 1)}} = & 7.26 - 1.75 \cdot \max(0, d/R - 0.12) + 2 \\ & \cdot \max(0, 0.12 - d/R) + 15.89 \cdot \max(0, C_v - 0.44) - 16.42 \\ & \cdot \max(0, 0.44 - C_v) + 0.47 \cdot \max(0, D_{gr} - 0.29) - 7.25 \\ & \cdot \max(0, \lambda - 0.3) - 16.03 \cdot \max(0, C_v - 0.01) + 3.7 \\ & \cdot \max(0, D_{gr} - 0.12) - 4.33 \cdot \max(0, D_{gr} - 0.08) + 0.43 \\ & \cdot \max(0, \lambda - 0.59) + 6.75 \cdot \max(0, \lambda - 0.28) + 1.67 \\ & \cdot \max(0, d/R - 0.07) \end{aligned} \quad (7)$$

270 May et al. (1996):

$$C_v = 0.0303 \left( \frac{D^2}{A} \right) \left( \frac{d}{D} \right)^{0.6} \left( 1 - \frac{V_t}{V_l} \right)^4 \left( \frac{V_l^2}{gd(S_s - 1)} \right)^{1.5} \quad (8)$$

271 Safari and Aksoy (2020):

$$\frac{V_l}{\sqrt{gd(S_s - 1)}} = 4.83 C_v^{0.09} \left( \frac{d}{R} \right)^{-0.32} D_{gr}^{-0.14} \left( \frac{P}{B} \right)^{0.20} \quad (9)$$

272 ANFIS-PSO:

273 No equation. The Matlab code can be found in Ebtehaj et al. (2019).

274 ELM:

$$\frac{V_l}{\sqrt{gd(S_s - 1)}} = \left[ \frac{1}{(1 + \exp(-\ln W \cdot \ln V + BHI))} \right]^T \cdot OutW \quad (10)$$

275 where  $\ln W$  and  $OutW$  are the input and output weights,  $BHI$  the bias of the hidden

276 neurons and  $\ln V$  the input variables (i.e.  $C_v$ ,  $d/R$ ,  $D^2/A$ ,  $R/D$ ,  $D_{gr}$ ,  $d/D$  and  $\lambda$ ). Full

277 details of the values chosen for each parameter are shown in Ebtehaj et al. (2020).

278 PSO:

$$\frac{V_l}{\sqrt{gd(S_s - 1)}} = 3.66 C_v^{0.16} \left( \frac{d}{R} \right)^{-0.40} \left( \frac{y_s}{Y} \right)^{-0.10} \quad (11)$$

279 LASSO:

$$\frac{V_l}{\sqrt{gd(S_s - 1)}} = 5.83 C_v^{0.144} \left( \frac{d}{R} \right)^{-0.305} \lambda^{-0.059} D_{gr}^{-0.169} \left( \frac{y_s}{D} \right)^{-0.104} \quad (12)$$

280 MGP:

$$\frac{V_l}{\sqrt{gd(S_s - 1)}} = 1.96 - 0.61\lambda - 0.51C_v + 1.18D_{gr}^{0.50}\lambda^{1.50} + 0.61\left(2C_v + \frac{d}{R}\right)^{0.50} - 2.45\left(\frac{d}{R}\right)^{1/8} \quad (13)$$

### 3.2.2. Performance Indices

The RF model performance is evaluated and compared to above ten models using three performance indicators. These are the Coefficient of Determination ( $R^2$ ), the Root Mean Square Error ( $RMSE$ ) and the Mean Absolute Percentage Error ( $MAPE$ ), defined as follows:

$$R^2 = 1 - \frac{\sum_{i=1}^n (F_{r_{OBS}}^* - F_{r_{MOD}})^2}{\sum_{i=1}^n (F_{r_{OBS}}^* - \overline{F_{r_{OBS}}^*})^2} \quad (14)$$

$$RMSE = \sqrt{\frac{1}{n} \sum_{i=1}^n (F_{r_{OBS}}^* - F_{r_{MOD}})^2} \quad (15)$$

$$MAPE = \frac{100}{n} \sum_{i=1}^n \left| \frac{F_{r_{OBS}}^* - F_{r_{MOD}}}{F_{r_{OBS}}^*} \right| \quad (16)$$

where  $F_{r_{OBS}}^*$  is the particle Froude number observed data,  $F_{r_{MOD}}$  the particle Froude number estimated by RF algorithm (or other predictive model),  $n$  the number of data and  $\overline{F_{r_{OBS}}^*}$  the mean of observed particle Froude number data.

The Coefficient of Determination measures the percentage of the model variance that can be explained. This coefficient varies between 0 and 1, with a value of 1 denoting a perfect match between observed and modelled data. The Root Mean Square Error measures the standard deviation of the residuals. Note that a value close to 0 indicates high model prediction accuracy. Finally, the Mean Absolute Percentage Error assesses the model prediction accuracy (i.e. bias) as a percentage of the observed value. Value of 0 indicates the perfect model where there are no differences between predictions and

observations.

#### 4. RESULTS

The results obtained by using the methodology shown in the previous section are presented in Table 3 and Table 4, for without deposited bed and deposited bed criteria, respectively. Graphically, these results are shown in Figure 5 and Figure 6. As shown in these tables, for the MARS, ANFIS-PSO, ELM and MGP models, the outliers of the particle Froude number (i.e.  $F_r^* < 0.00$  and  $F_r^* > 20.00$ ) were removed. This is because these models can produce extreme values (e.g.  $F_r^* = -58.67$  or  $F_r^* = 163.59$ , among others) that misrepresent the model comparison when evaluating the performance indices.

#### [Table 3 near here]

As it can be seen from Table 3, Random Forest model shows a better generalisation capacity than other models shown, as demonstrated in high prediction accuracy observed for all available datasets ( $0.88 > R^2 > 0.98$ ,  $0.24 > RMSE > 0.73$  and  $4.36\% > MAPE > 11.09\%$ ). The following observations can be made from the performance of the other models evaluated:

- EPR-MOGA, similarly to RF, shows good results but has inferior accuracy in large sewer pipes ( $R^2 = 0.86$ ,  $RMSE = 1.03$  and  $MAPE = 11.31\%$ ). In addition, EPR-MOGA model shows limitations for predicting the particle Froude number in non-circular sections (as shown in the Mayerle (1988) rectangular data). This equation shows good extrapolation capabilities because of the inclusion of the pipe slope as input feature for the self-cleansing prediction.
- GEP shows acceptable results ( $0.79 > R^2 > 0.87$ ,  $0.66 > RMSE > 0.89$  and  $11.45\% > MAPE > 22.33\%$ ) for the datasets used for its development in circular channels (Ab Ghani, 1993; Mayerle, 1988; Vongvisessomjai et al., 2010) and poor



performance for other datasets ( $0.00 > R^2 > 0.76$ ,  $1.00 > RMSE > 1.95$  and  $14.35\% > MAPE > 37.92\%$ ). This model presents good performance for large sewer pipes. In contrast, for non-circular channels the model quickly loss accuracy.

- According to Safari (2019), MARS model was developed by using the experimental data collected by Mayerle (1988) (in both circular and rectangular channels), May (1993), Ab Ghani (1993) and Vongvisessomjai et al. (2010). As a result, this model shows acceptable performance for these datasets ( $0.49 > R^2 > 0.87$ ,  $0.81 > RMSE > 1.15$  and  $13.63\% > MAPE > 28.08\%$ ) but poor performance for the remaining datasets ( $R^2 = 0.00$ ,  $1.48 > RMSE > 2.88$  and  $29.14\% > MAPE > 51.28\%$ ). Based on the above, and compared to the RF model, limited extrapolation capabilities are identified for the MARS model.

- May et al. (1996) is the best regression-based equation reported in the literature (Ackers et al., 2001; Ebtehaj et al., 2014), as it was developed using several experimental datasets. This is the equation proposed by the Construction Industry Research and Information Association (CIRIA) for designing self-cleansing sewer pipes transporting coarser granular material as bedload (Ackers et al., 2001). This model shows good performance for pipe diameters less than 500 mm ( $0.83 > R^2 > 0.99$ ,  $0.13 > RMSE > 0.82$  and  $2.38\% > MAPE > 11.61\%$ ). In contrast, limited extrapolation for large sewer pipes is identified as the low performance indices values obtained ( $R^2 = 0.00$ ,  $RMSE = 4.88$  and  $MAPE = 48.97\%$ ). This equation shows better performance than the RF model when compared to data from Vongvisessomjai et al. (2010), but lower accuracy when applied to the rest of the datasets.

- Safari and Aksoy (2020) model is a competitive equation for predicting the self-cleansing velocity in both circular and non-circular channels. This model shows

similar but inferior performance to EPR-MOGA model in small sewer pipes ( $0.67 > R^2 > 0.97$ ,  $0.25 > RMSE > 1.12$  and  $7.90\% > MAPE > 15.60\%$ ), but in large sewers the accuracy is quickly lost ( $R^2 = 0.34$ ,  $RMSE = 2.26$  and  $MAPE = 23.46\%$ ). In contrast, this model outperforms the results, compared to other regression models (EPR-MOGA, GEP and MARS) and ML/AI models (ANFIS-PSO and ELM), in non-circular channels ( $R^2 = 0.87$ ,  $RMSE = 0.66$  and  $MAPE = 13.41\%$ ), which is a competitive performance compared to the RF model ( $R^2 = 0.89$ ,  $RMSE = 0.61$  and  $MAPE = 10.05\%$ ). This is because of the inclusion of the  $P/B$  relation as explanatory variable for predicting the particle Froude number. This model is competitive and shows good generalisation of the problem for designing sewers under the non-deposition without deposited bed criterion.

- According to Ebtehaj et al. (2019), ANFIS-PSO model was developed by using the experimental data collected by Ab Ghani (1993), Ota (1999) and Vongvisessomjai et al. (2010). As a result, this model shows good performance for these datasets ( $0.88 > R^2 > 0.97$ ,  $0.22 > RMSE > 0.74$  and  $3.62\% > MAPE > 10.34\%$ ). In large sewers and non-circular channels, the model losses accuracy ( $R^2 = 0.00$ ,  $2.74 > RMSE > 3.01$  and  $30.56\% > MAPE > 45.28\%$ ). This model produces some extreme values when the particle Froude number is calculated, especially in the Montes et al. (2020b) dataset. The RF model generates better results compared to this model.
- ELM was trained with the same dataset used for the ANFIS-PSO model. Not satisfactory results are obtained when this model is applied on the dataset considered in this study ( $0.00 > R^2 > 0.55$ ,  $0.90 > RMSE > 3.1$  and  $19.54\% > MAPE > 39.30\%$ ). Same comments, as mentioned above for the ANFIS-PSO model, can be shown here.

[Figure 5 near here]

[Table 4 near here]

According to the results shown in Table 4 (deposited bed criterion), RF model outperforms the other models for the entire considered dataset. This model shows good accuracy levels ( $0.84 > R^2 > 0.98$ ,  $0.32 > RMSE > 0.81$  and  $4.70\% > MAPE > 12.10\%$ ) for all the range of variation of the hydraulics and sediment characteristics. Comments related to the other models studied are as follows:

- PSO model was developed by using the experimental data collected by El-Zaemey (1991), Perrusquía (1991), May (1993) and Ab Ghani (1993). As a result, this model shows good performance for these datasets ( $0.56 > R^2 > 0.78$ ,  $0.49 > RMSE > 1.32$  and  $10.15\% > MAPE > 16.26\%$ ). However, when the model is compared to the data collected in the large sewer pipe, the accuracy quickly decreases ( $R^2 = 0.00$ ,  $RMSE = 3.06$  and  $MAPE = 21.05\%$ ).
- LASSO model reports good accuracy levels for all the datasets considered ( $0.62 > R^2 > 0.83$ ,  $0.50 > RMSE > 1.56$  and  $10.36\% > MAPE > 14.26\%$ ). However, the accuracy is still inferior compared to the RF model. This model shows good extrapolation capabilities and generalisation of the problem.
- MGP was developed by using the same experimental datasets of the PSO model. This model shows less accuracy compared to the PSO model ( $0.00 > R^2 > 0.54$ ,  $1.08 > RMSE > 5.54$  and  $13.07\% > MAPE > 58.79\%$ ). In large sewer pipes, the model shows poor performance. In contrast to other models, the MGP was developed by using normalised values. Based on this, the range of variation used for training the model can potentially affect the final form/structure of the final expression shown by the MGP.

[Figure 6 near here]

RF accuracy shown in the Montes et al. (2020b) data is especially important due to the relative sediment thickness ( $y_s/D$ ) used at laboratory scale in that study. As Table 1 shows, the sediment thickness used at laboratory scale ranging from 0.8 mm (for Montes et al. (2020b) data) to 129.6 mm (for May (1993) data), i.e. the variation of  $y_s/D$  is from 1.1% to 20.0% of the pipe diameter. Values of  $y_s/D = 20\%$  is an unrealistic consideration since the optimal sediment thickness design has been defined as 1% of the pipe diameter (May et al., 1989; Safari and Shirzad, 2019). Data collected by Montes et al. (2020b) seem to be the closer representation of the real conditions found in sewer systems. Based on this, RF is the model that best predicts the self-cleansing velocity for data close to real conditions.

#### 4.1. Variable importance

RF model input variable importance is presented in Figure 7. As shown in this figure, for both non-deposition criteria the most important variable is the volumetric sediment concentration, followed by the dimensionless grain size and the relative grain size. This result is consistent with previous findings reported in the literature (Ackers et al., 2001; Ebtehaj et al., 2020). Less important parameters for predicting the particle Froude number and thus the self-cleansing velocity, are the relative sediment thickness and the channel friction factor, for the deposited bed criterion.

Parameter importance shown by EPR-MOGA, Safari and Aksoy (2020), PSO and LASSO is quite different. In these techniques, the most important parameter is the relative grain size due to the highest values of the regression coefficients  $\left(\left(\frac{d}{R}\right)^{-c}; 0.305 < c < 0.58\right)$ , as shown in Eq. (5), Eq. (9), Eq. (11) and Eq. (12). The parameter importance for the GEP, MARS and MGP model is less intuitive because of the form of the equations,

as shown in Eq. (6), Eq. (7) and Eq. (13), which include logarithmic and inverse tangent functions for calculating the particle Froude number. Less comparable are the results shown by ANFIS-PSO and ELM since no practical equation is provided.

**[Figure 7 near here]**

Based on the above results shown in Figure 7, a good estimate of the volumetric sediment concentration seems to be essential for increasing the accuracy of the calculation of the particle Froude number and consequently the minimum self-cleansing velocity for both non-deposition criteria. In addition, hydraulic characteristics of the pipe (defined by the hydraulic radius) and the sediment characteristics (i.e. particle diameter and specific gravity) are proportionally important for model performance.

## **5. DISCUSSION**

The prediction of self-cleansing conditions in sewers remains a challenge despite multiple models and equations developed and reported in the literature. Existing regression-based equations and AI/ML models show limited generalisation capabilities and overfitting problems. In this paper, a new approach for addressing these issues is proposed by using the Random Forest method.

Due to the nature of the RF method, where the model variance is reduced by averaging the results from an ensemble of decision trees, the risk of overfitting is low. By using a reduced number of input features for constructing each decision tree in the forest, the correlation between base trees is avoided. This is an improvement of the method compared to a single decision tree, which can be overtrained (i.e. the tree learns the noise from the training data) and thus shows poor performance in the testing dataset.

RF model showed good generalisation capabilities when the whole dataset is divided into 75% for the training stage and 25% for the testing stage. For this percentage of split data, the testing error presented a low variance. In contrast, by increasing the

number of data used in the training stage (e.g. 95% of the whole data) the testing error showed high variance, which is an indicator of an over-trained model with limited extrapolation capabilities (as shown in Figure 3b). Therefore, choosing the right percentage split is critical to avoid model overfitting.

Variable importance analysis showed that the volumetric sediment concentration is the most relevant feature for predicting the self-cleansing velocity in practice for both non-deposition criteria, followed by the dimensionless grain size. The self-cleansing prediction is no conditioned by the channel material, as the low variable importance shown by the channel friction factor.

RF results are compared to existing models reported in the literature and showed better performance for the whole dataset for both non-deposition without and with deposited bed criteria. This is explained by several factors, such as:

- RF is able to better capture the non-linearity in the data compared to linear regression models (i.e. regression-based models proposed by May et al. (1996) and Safari and Aksory (2020)). The RF model also better captures complex interactions between features. This is because of RF model's ability to capture effectively non-linear patterns in data.
- RF showed a good bias-variance trade-off (i.e. low bias and low variance) for both non-deposition criteria. In contrast, existing non-regression models reported in the literature (i.e. MARS, ANFIS-PSO and ELM), and compared to the RF model in this paper, in some cases presented low bias and high variance (i.e. overfitting) for the non-deposition without deposited bed criterion, as shown in Figure 5. For the non-deposition with deposited bed criterion, the existing models (i.e. PSO, LASSO and MGP) showed high bias, since these models systematically

underestimate the particle Froude number in the testing dataset (as shown in Figure 6).

- The range of variation used for training and testing the RF model is much larger than the dataset used in the literature for developing the existing predictive models. For example, the ANFIS-PSO and ELM were trained and testing with the Ab Ghani (1993), Ota (1999) and Vongvisessomjai et al. (2010) data (i.e. 290 data approx.). Given this, the RF model developed here is able to predict the particle Froude number for a larger range of variation of the input conditions. An example of this is shown in Figure 6 where the existing models reported for the non-deposition with deposited bed criterion underestimate the particle Froude number for values above 9.0 ( $F_r^* > 9.0$ ).

Despite the RF presented in this study outperforms the existing models reported in the literature, further tests with data collected in real sewers should be conducted. The cohesive effects of the deposited material must be included for future developments. Finally, further evaluation of the performance of the model in trapezoidal, ovoid, or U-shape channels should be carried out to check the applicability of the model under these channel characteristics.

## 6. CONCLUSIONS

Random Forest based model was developed for predicting the self-cleansing velocity under the concept of non-deposition. This model was implemented using the experimental benchmark data reported in the literature. The RF model was compared to the following ten literature models: EPR-MOGA, MARS, MGP, ANFIS-PSO, ELM, LASSO, GEP and PSO, and two regression-based equations proposed by May et al. (1996) and Safari and Aksoy (2020).

The following conclusions are made based on the results obtained:

- (1) Random Forest model is able to predict the particle Froude number (i.e. minimum self-cleansing velocity) for the non-deposition self-cleansing design criteria with high accuracy on validation (i.e. unseen) data. This is due to the ability of RF to better generalise the analysed data, i.e. the ability to avoid model overfitting.
- (2) RF model prediction accuracy is consistently superior to ten other literature models considered here. This is likely due to the reason mentioned above but also the capability to better capture the complex interactions between input variables when compared to other models considered in this paper. This is especially relevant for the non-deposition with deposited bed case where the accuracy of RF model predictions is substantially higher than in other models (i.e. LASSO, MGP and PSO models).
- (3) The volumetric sediment concentration is the most important input variable for predicting the self-cleansing velocity in sewer pipes. A good characterisation of this parameter seems to be essential for improving the design of new self-cleansing sewers.

Based on the above, RF can be used for predicting self-cleansing velocity with high accuracy, especially for large sewer pipes with the presence of deposited bed. This technique can be used for designing self-cleansing sewer systems.

Further testing of the RF and other self-cleansing models in real sewer systems is required to further validate these models in those circumstances and ensure their applicability in engineering practice.

## **7. SUPPLEMENTARY MATERIAL**

Data used for training and testing the Random Forest method is shown in Table S1 and



Table S2 for non-deposition without and with deposited bed, respectively. In addition, an example of one of the decision trees considered by the RF method is shown in Figure S1.

## FUNDING

This research did not receive any specific grant from funding agencies in the public, commercial, or not-for-profit sectors.

## REFERENCES

- Ab Ghani, A., 1993. Sediment Transport in Sewers. PhD thesis, University of Newcastle upon Tyne, Newcastle upon Tyne, UK.
- Ackers, J., Butler, D., Leggett, D., May, R., 2001. Designing Sewers to Control Sediment Problems, in: Urban Drainage Modeling. ASCE, Orlando, FL, pp. 818–823. [https://doi.org/10.1061/40583\(275\)77](https://doi.org/10.1061/40583(275)77)
- Breiman, L., 2001. Random Forests. Mach. Learn. 45, 5–32. <https://doi.org/10.1023/A:1010933404324>
- Ebtehaj, I., Bonakdari, H., 2016a. Bed Load Sediment Transport in Sewers at Limit of Deposition. Sci. Iran. 23 (3), 907–917. <https://doi.org/10.24200/sci.2016.2169>
- Ebtehaj, I., Bonakdari, H., 2016b. A support vector regression-firefly algorithm-based model for limiting velocity prediction in sewer pipes. Water Sci. Technol. 73 (9), 2244–2250. <https://doi.org/10.2166/wst.2016.064>
- Ebtehaj, I., Bonakdari, H., 2013. Evaluation of sediment transport in sewer using artificial neural network. Eng. Appl. Comput. Fluid Mech. 7 (3), 382–392. <https://doi.org/10.1080/19942060.2013.11015479>
- Ebtehaj, I., Bonakdari, H., Es-Haghi, M., 2019. Design of a Hybrid ANFIS–PSO Model to Estimate Sediment Transport in Open Channels. Iran. J. Sci. Technol. Trans. 44 (4), 851–857. <https://doi.org/10.1007/s40996-018-0218-9>
- Ebtehaj, I., Bonakdari, H., Safari, M., Gharabaghi, B., Zaji, A., Riahi Madavar, H., Sheikh Khozani, Z., Es-haghi, M., Shishegaran, A., Danandeh Mehr, A., 2020. Combination of sensitivity and uncertainty analyses for sediment transport modeling in sewer pipes. Int. J. Sediment Res. 35 (2), 157–170. <https://doi.org/10.1016/j.ijsrc.2019.08.005>

544 Ebtehaj, I., Bonakdari, H., Sharifi, A., 2014. Design criteria for sediment transport in  
545 sewers based on self-cleansing concept. *J. Zhejiang Univ. Sci. A* 15 (11), 914-  
546 924. <https://doi.org/10.1631/jzus.a1300135>

547 El-Zaemey A., 1991. Sediment Transport over Deposited Beds in Sewers. PhD thesis,  
548 University of Newcastle upon Tyne, Newcastle upon Tyne, UK.

549 Hastie, T., Tibshirani, R., Friedman, J., 2009. The Elements of Statistical Learning: Data  
550 Mining, Inference, and Prediction. Springer, New York, USA.  
551 <https://doi.org/10.1007/978-0-387-84858-7>

552 Kargar, K., Safari, M., Mohammadi, M., Samadianfard, S., 2019. Sediment transport  
553 modeling in open channels using neuro-fuzzy and gene expression programming  
554 techniques. *Water Sci. Technol.* 79 (12), 2318–2327.  
555 <https://doi.org/10.2166/wst.2019.229>

556 Liaw, A., Wiener, M., 2002. Classification and Regression by randomForest. *R News* 2  
557 (3), 18–22.

558 May R., 1993. Sediment Transport in Pipes and Sewers with Deposited Beds. Report SR  
559 320, HR Wallingford, Oxfordshire, UK.

560 May R., Ackers, J., Butler, D., John, S., 1996. Development of design methodology for  
561 self-cleansing sewers. *Water Sci. Technol.* 33 (9), 195–205.  
562 [https://doi.org/10.1016/0273-1223\(96\)00387-3](https://doi.org/10.1016/0273-1223(96)00387-3)

563 May R., Brown P., Hare G., Jones K., 1989. Self-Cleansing Conditions for Sewers  
564 Carrying Sediment. Report SR 221, HR Wallingford, Oxfordshire, UK.

565 Mayerle R., 1988. Sediment Transport in Rigid Boundary Channels. PhD thesis,  
566 University of Newcastle upon Tyne, Newcastle upon Tyne, UK.

567 Merritt, L., Enfinger, K., 2019. Tractive Force: A Key to Solids Transport in Gravity  
568 Flow Drainage Pipes, in: *Pipelines 2019*. ASCE, Nashville, TN, pp. 349–358.

569 Montes, C., Berardi, L., Kapelan, Z., Saldarriaga, J., 2020a. Predicting bedload sediment  
570 transport of non-cohesive material in sewer pipes using evolutionary polynomial  
571 regression – multi-objective genetic algorithm strategy. *Urban Water J.* 17 (2),  
572 154–162. <https://doi.org/10.1080/1573062X.2020.1748210>

573 Montes, C., Kapelan, Z., Saldarriaga, J., 2019. Impact of Self-Cleansing Criteria Choice  
574 on the Optimal Design of Sewer Networks in South America. *Water* 11 (6), 1148.  
575 <https://doi.org/10.3390/w11061148>

576 Montes, C., Vanegas, S., Kapelan, Z., Berardi, L., Saldarriaga, J., 2020b. Non-deposition  
 577 self-cleansing models for large sewer pipes. *Water Sci. Technol.* 81 (3), 606-621.  
 578 <https://doi.org/10.2166/wst.2020.154>  
 579 Nalluri, C., Ab Ghani, A., 1996. Design options for self-cleansing storm sewers. *Water*  
 580 *Sci. Technol.* 33 (9), 215–220. [https://doi.org/10.1016/0273-1223\(96\)00389-7](https://doi.org/10.1016/0273-1223(96)00389-7)  
 581 Ota J., 1999. Effect of Particle Size and Gradation on Sediment Transport in Storm  
 582 Sewers. PhD thesis, University of Newcastle upon Tyne, Newcastle upon Tyne,  
 583 UK.  
 584 Perrusquía, G., 1991. Bedload Transport in Storm Sewers: Stream Traction in Pipe  
 585 Channels. PhD thesis, Chalmers University of Technology, Gothenburg, Sweden.  
 586 Roushangar, K., Ghasempour, R., 2017. Estimation of bedload discharge in sewer pipes  
 587 with different boundary conditions using an evolutionary algorithm. *Int. J.*  
 588 *Sediment Res.* 32 (4), 564–574. <https://doi.org/10.1016/j.ijsrc.2017.05.007>  
 589 Safari, M., 2019. Decision tree (DT), generalized regression neural network (GR) and  
 590 multivariate adaptive regression splines (MARS) models for sediment transport  
 591 in sewer pipes. *Water Sci. Technol.* 79 (6), 1113-1122.  
 592 <https://doi.org/10.2166/wst.2019.106>  
 593 Safari, M., Danandeh Mehr, A., 2018. Multigene genetic programming for sediment  
 594 transport modeling in sewers for conditions of non-deposition with a bed deposit.  
 595 *Int. J. Sediment Res.* 33 (3), 262-270. <https://doi.org/10.1016/j.ijsrc.2018.04.007>  
 596 Safari, M., Mohammadi, M., Ab Ghani, A., 2018. Experimental Studies of Self-Cleansing  
 597 Drainage System Design: A Review. *J. Pipeline Syst. Eng. Pract.* 9 (4), 04018017.  
 598 [https://doi.org/10.1061/\(ASCE\)PS.1949-1204.0000335](https://doi.org/10.1061/(ASCE)PS.1949-1204.0000335)  
 599 Safari, M., Shirzad, A., 2019. Self-cleansing design of sewers: Definition of the optimum  
 600 deposited bed thickness. *Water Environ. Res.* 91 (5), 407–416.  
 601 <https://doi.org/10.1002/wer.1037>  
 602 Safari, M., Shirzad, A., Mohammadi, M., 2017. Sediment transport modeling in deposited  
 603 bed sewers: Unified form of May's equations using the particle swarm  
 604 optimization algorithm. *Water Sci. Technol.* 76 (4), 992–1000.  
 605 <https://doi.org/10.2166/wst.2017.267>  
 606 Safari, M., 2020. Hybridization of multivariate adaptive regression splines and random  
 607 forest models with an empirical equation for sediment deposition prediction in

608 open channel flow. *J. Hydrol.* 590 (November 2020), 125392.  
 609 <https://doi.org/10.1016/j.jhydrol.2020.125392>  
 610 Safari, M., Aksoy, H., 2020. Experimental analysis for self-cleansing open channel  
 611 design. *J. Hydraul. Res.* 1-12. <https://doi.org/10.1080/00221686.2020.1780501>  
 612 Tyralis, H., Papacharalampous, G., & Langousis, A. 2019 A Brief Review of Random  
 613 Forests for Water Scientists and Practitioners and Their Recent History in Water  
 614 Resources. *Water*, 11(5), 910. <https://doi.org/10.3390/w11050910>  
 615 Vongvisessomjai, N., Tingsanchali, T., & Babel, M. 2010 Non-deposition design criteria  
 616 for sewers with part-full flow. *Urban Water Journal*, 7(1), 61–77.  
 617 <https://doi.org/10.1080/15730620903242824>  
 618 Zendehboudi, S., Rezaei, N., & Lohi, A. 2018 Applications of hybrid models in chemical,  
 619 petroleum, and energy systems: A systematic review. *Applied Energy*, 228(2018),  
 620 2539–2566. <https://doi.org/10.1016/j.apenergy.2018.06.051>

621 Table 1. Data used for implementing data mining and regression models.

Reference	Non-deposition criterion	No. of runs	Pipe diameter or bottom width (mm)	Flow Velocity (m/s)	Pipe slope (%)	Sediment Concentration (ppm)	Sediment thickness bed (mm)
Mayerle (1988) circular channel	Without deposited bed	106	152	0.37 - 1.10	0.13 - 0.56	20.0 - 1275.0	-
Mayerle (1988) rectangular channel	Without deposited bed	105	311.5 and 462.3	0.41 - 1.04	0.09 - 0.64	14.0 - 1568.0	-
Ab Ghani (1993)	Without deposited bed	221	154, 305 and 405	0.24 - 1.22	0.04 - 2.56	0.8 - 1450.0	-
Ota (1999)	Without deposited bed	36	305	0.39 - 0.74	0.2	4.2 - 59.4	-
Vongvisessomjai et al. (2010)	Without deposited bed	45	100 and 150	0.24 - 0.63	0.20 - 0.60	4.0 - 90.0	-
Montes et al. (2020a)	Without deposited bed	44	242	0.24 - 1.05	0.20 - 0.80	0.3 - 875.7	-
Montes et al. (2020b)	Without deposited bed	107	595	0.41 - 1.41	0.04 - 3.43	1.3 - 19957.0	-
El-Zaemey (1991)	With deposited bed	290	305	0.39 - 0.96	0.05 - 0.44	7.0 - 917.0	47.0 - 120.0
Perrusquía (1991)	With deposited bed	38	225	0.29 - 0.67	0.20 - 0.60	18.7 - 408.0	45.0 - 90.0
Ab Ghani (1993)	With deposited bed	26	450	0.49 - 1.33	0.07 - 0.47	21.0 - 1259.0	52.0 - 108.0
May (1993)	With deposited bed	46	450	0.39 - 1.14	0.07 - 0.97	3.5 - 823.0	57.6 - 129.6
Montes et al. (2020b)	With deposited bed	54	595	0.73 - 1.53	0.46 - 5.42	389.0 - 10275.0	0.8 - 6.6

622

623 Table 2. Variation of the data for training and testing the RF model.

Non-deposition criterion	Stage	No. of runs	Channel geometry (mm)	Flow Velocity (m/s)	Pipe slope (%)	Sediment Concentration (ppm)	Sediment thickness bed (mm)
Without deposited bed	Training	498	$D = 100.0 - 595.0$ $W = 311.5 - 462.3$	0.237 - 1.41	0.04 - 3.43	0.53 - 19957	-
	Testing	166	$D = 100.0 - 595.0$ $W = 311.5 - 462.3$	0.237 - 1.24	0.04 - 2.74	1.00 - 13840	-
With deposited bed	Training	340	$D = 225 - 595$	0.294 - 1.53	0.05 - 5.42	3.50 - 10274	0.78 - 129.6
	Testing	114	$D = 225 - 595$	0.319 - 1.28	0.05 - 2.58	17.00 - 9101	1.78 - 120.0

624

Table 3. Accuracy of self-cleansing models for without deposited bed criterion using performance indices for training and testing dataset. Bolded values show best performance model.

Dataset	Performance Index	Model							
		RF	EPR-MOGA	GEP	MARS	May et al. (1996) <sup>1</sup>	Safari and Aksoy (2020)	ANFIS-PSO	ELM
Training	$R^2$	<b>0.98</b>	0.90	0.75	0.00	0.27	0.74	0.51*	0.30*
	RMSE	<b>0.33</b>	0.76	1.22	2.55	2.17	1.25	1.69*	1.95*
	MAPE (%)	<b>4.88</b>	11.54	23.52	34.16	17.49	17.21	19.32*	29.76*
Testing	$R^2$	<b>0.91</b>	0.86	0.69	0.00	0.09	0.74	0.40*	0.32*
	RMSE	<b>0.73</b>	0.88	1.33	2.55	2.27	1.21	1.84*	1.92*
	MAPE (%)	<b>11.09</b>	12.35	26.43	36.57	19.15	17.24	20.95*	29.82*
Mayerle (1988) circular	$R^2$	<b>0.96</b>	0.89	0.87	0.87	0.87	0.75	0.80*	0.42
	RMSE	<b>0.45</b>	0.75	0.81	0.81	0.82	1.12	1.00*	1.71
	MAPE (%)	<b>5.62</b>	8.90	14.77	14.03	11.49	14.91	17.92*	26.75
Mayerle (1988) rectangular	$R^2$	<b>0.93</b>	0.38	0.30	0.81	-	0.87	0.00	0.47
	RMSE	<b>0.49</b>	1.44	1.54	0.81	-	0.66	2.74	1.33
	MAPE (%)	<b>8.49</b>	28.97	33.00	15.51	-	13.14	45.28	20.75
Ab Ghani (1993)	$R^2$	<b>0.97</b>	0.96	0.83	0.72	0.90	0.81	0.88	0.38
	RMSE	<b>0.36</b>	0.43	0.89	1.15	0.67	0.94	0.74	1.69
	MAPE (%)	<b>5.94</b>	9.35	22.33	28.08	10.32	15.60	10.34	23.96
Ota (1999)	$R^2$	0.97	<b>0.98</b>	0.44	0.00	0.96	0.97	0.97	0.55
	RMSE	0.24	<b>0.20</b>	1.00	1.48	0.27	0.25	0.22	0.90
	MAPE (%)	<b>5.55</b>	6.90	37.92	51.28	7.78	7.90	6.46	19.54
Vongvisessomjai et al. (2010)	$R^2$	0.88	0.95	0.79	0.49	<b>0.99</b>	0.71	0.97	0.00
	RMSE	0.49	0.33	0.66	1.03	<b>0.13</b>	0.78	0.24	1.59
	MAPE (%)	6.56	5.78	11.45	13.63	<b>2.38</b>	13.34	3.62	28.50
Montes et al. (2020a)	$R^2$	0.96	<b>0.98</b>	0.00	0.00	0.83	0.67	0.77*	0.00
	RMSE	0.31	<b>0.25</b>	1.64	2.37	0.67	0.94	0.75*	1.85
	MAPE (%)	<b>4.36</b>	4.94	28.15	49.73	11.61	15.39	12.39*	33.96
Montes et al. (2020b)	$R^2$	<b>0.94</b>	0.86	0.76	0.00*	0.00	0.34	0.00*	0.00*
	RMSE	<b>0.70</b>	1.03	1.37	2.88*	4.88	2.26	3.01*	3.10*
	MAPE (%)	<b>7.33</b>	11.31	14.35	29.14*	48.97	23.44	30.56*	39.30*

<sup>1</sup> Model not valid for non-circular channels

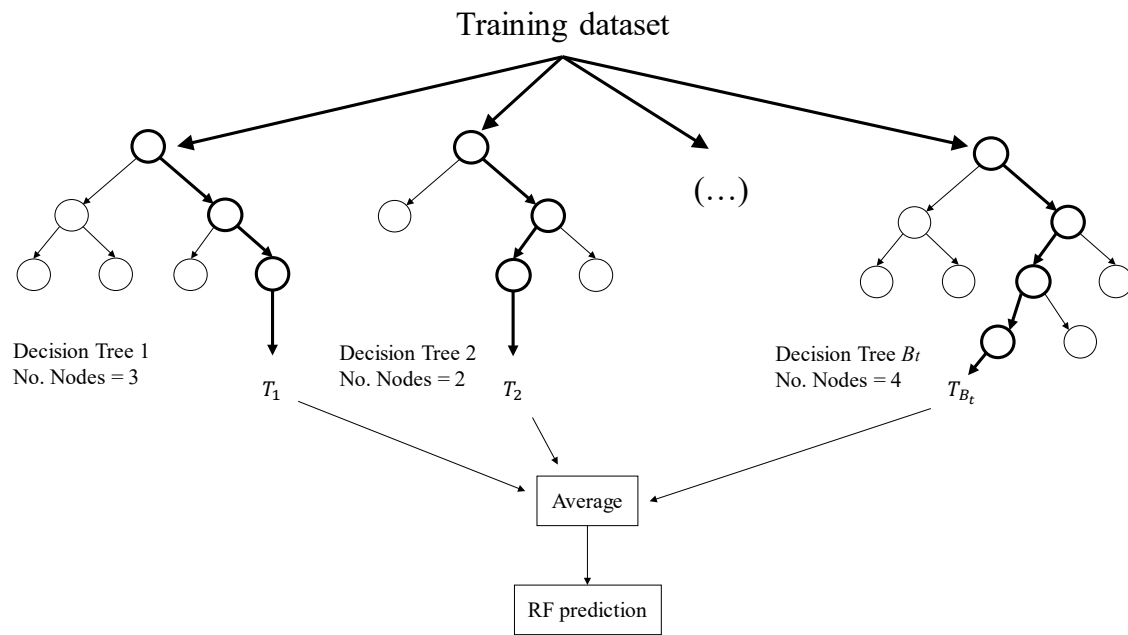
\* Outliers removed

Table 4. Accuracy of self-cleansing models for deposited bed criterion using performance indices for training and testing dataset. Bolded values show best performance model.

Dataset	Performance Index	Model			
		RF	PSO	LASSO	MGP
Training	$R^2$	<b>0.98</b>	0.75	0.82	0.51*
	$RMSE$	<b>0.32</b>	1.30	1.13	1.69*
	$MAPE$ (%)	<b>4.70</b>	14.36	13.07	28.78*
Testing	$R^2$	<b>0.91</b>	0.70	0.83	0.29*
	$RMSE$	<b>0.80</b>	1.47	1.10	2.19*
	$MAPE$ (%)	<b>12.10</b>	15.94	12.59	31.36*
El-Zaemey (1991)	$R^2$	<b>0.94</b>	0.78	0.83	0.54
	$RMSE$	<b>0.38</b>	0.76	0.66	1.08
	$MAPE$ (%)	<b>6.49</b>	14.28	11.97	30.19
Perrusquía (1991)	$R^2$	<b>0.84</b>	0.65	0.62	0.00
	$RMSE$	<b>0.33</b>	0.49	0.50	1.29
	$MAPE$ (%)	<b>7.07</b>	10.15	12.05	30.58
Ab Ghani (1993)	$R^2$	<b>0.91</b>	0.56	0.74	0.51
	$RMSE$	<b>0.60</b>	1.32	1.01	1.40
	$MAPE$ (%)	<b>6.13</b>	16.26	11.19	13.07
May (1993)	$R^2$	<b>0.90</b>	0.63	0.64	0.54
	$RMSE$	<b>0.62</b>	1.18	1.16	1.31
	$MAPE$ (%)	<b>6.50</b>	13.47	14.26	14.21
Montes et al. (2020a)	$R^2$	<b>0.93</b>	0.00	0.73	0.00*
	$RMSE$	<b>0.81</b>	3.06	1.56	5.54*
	$MAPE$ (%)	<b>6.84</b>	21.05	10.36	58.79*

\* Outliers removed





633

634 Figure 1. Simplified conceptual diagram of the RF method.

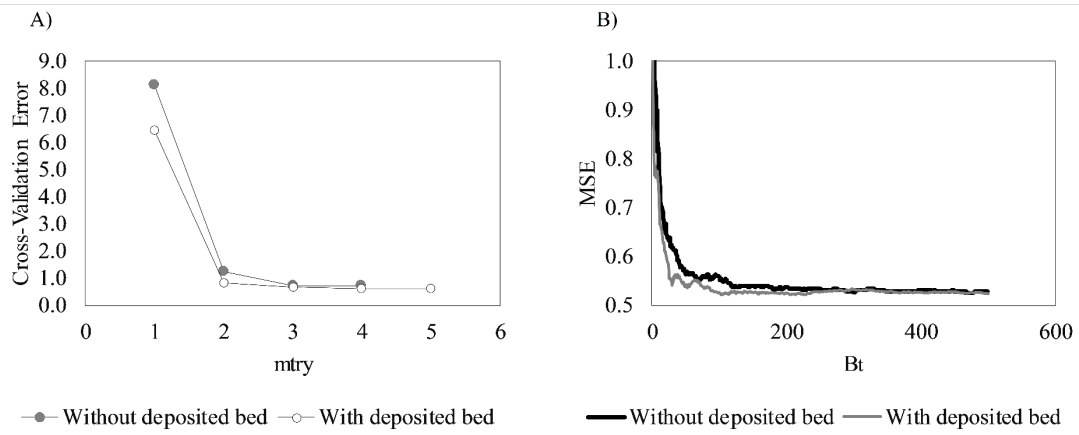


Figure 2. Selection of the optimal Random Forest parameters.

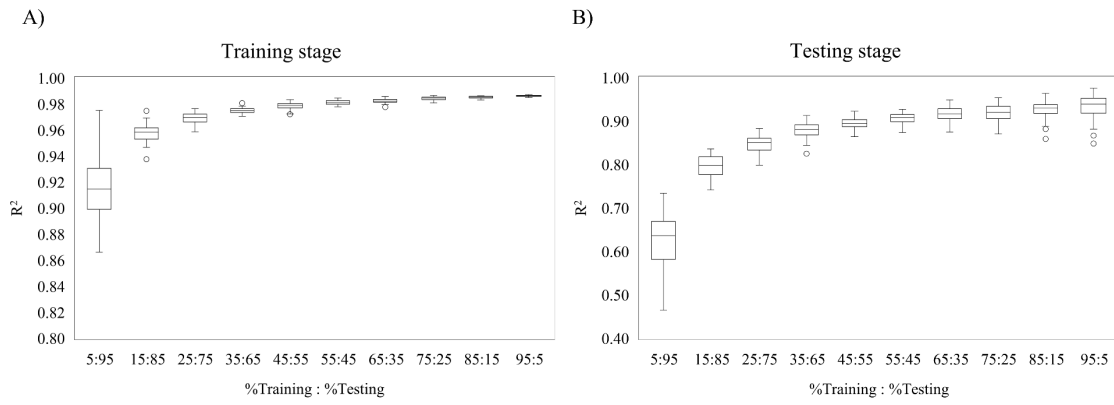


Figure 3. Variation of the training and testing error using different combination of percentages between the training and testing dataset. A) Training stage and B) Testing stage.

```

1  #####Random Forest model
2
3  library(randomForest)
4
5  #load data shown in Table S1 (without deposited bed)
6  #or Table S2 (with deposited bed)
7  #Please remove the "Fr* prediction RF" column
8
9  data=read.csv("Fullldata.csv",header=TRUE,sep=",")
10
11  set.seed(4260)
12
13  train=sample(1:nrow(data),nrow(data)*0.75)
14  test=data[-train,]
15  train=data[train,]
16
17  #Run Random Forest method
18  #Use ntree = 471 and mtry = 3 for without deposited bed
19  #Use ntree = 229 and mtry = 4 for with deposited bed
20
21  rf=randomForest(Frp~.,data=train,
22                  localImp=TRUE,importance=TRUE,
23                  mtry=3,ntree=471)
24
25  #RF Prediction in training and testing dataset
26
27  rf.pred.train=predict(rf,newdata=train)
28  rf.pred.test=predict(rf,newdata=test)
29
30  #Use function predict() to calculate the particle
31  #Froude number using other datasets. Use the same
32  #data frame headers.

```

641

642 Figure 4. Random Forest code to calculate the particle Froude number in sewer pipes.

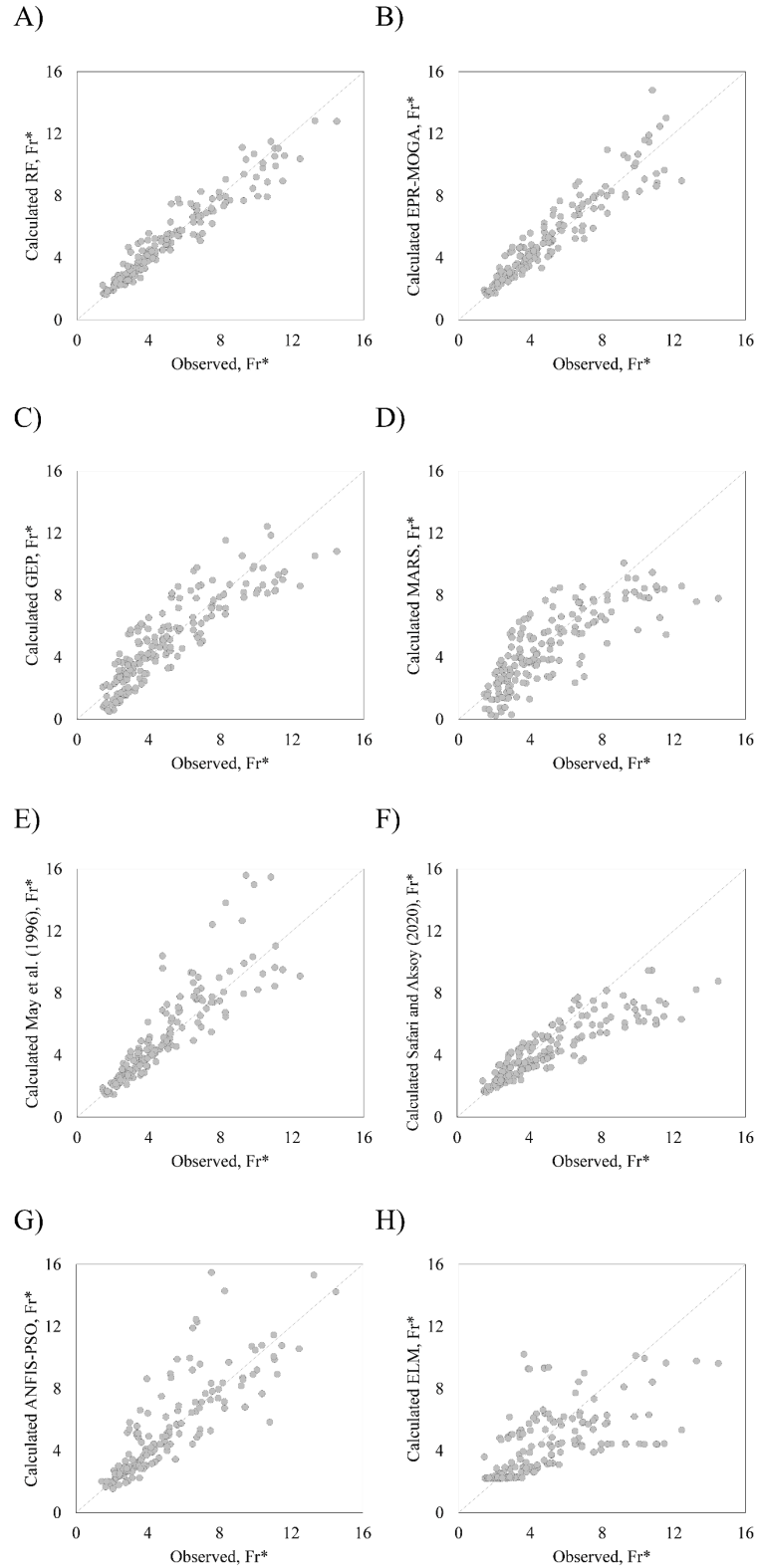
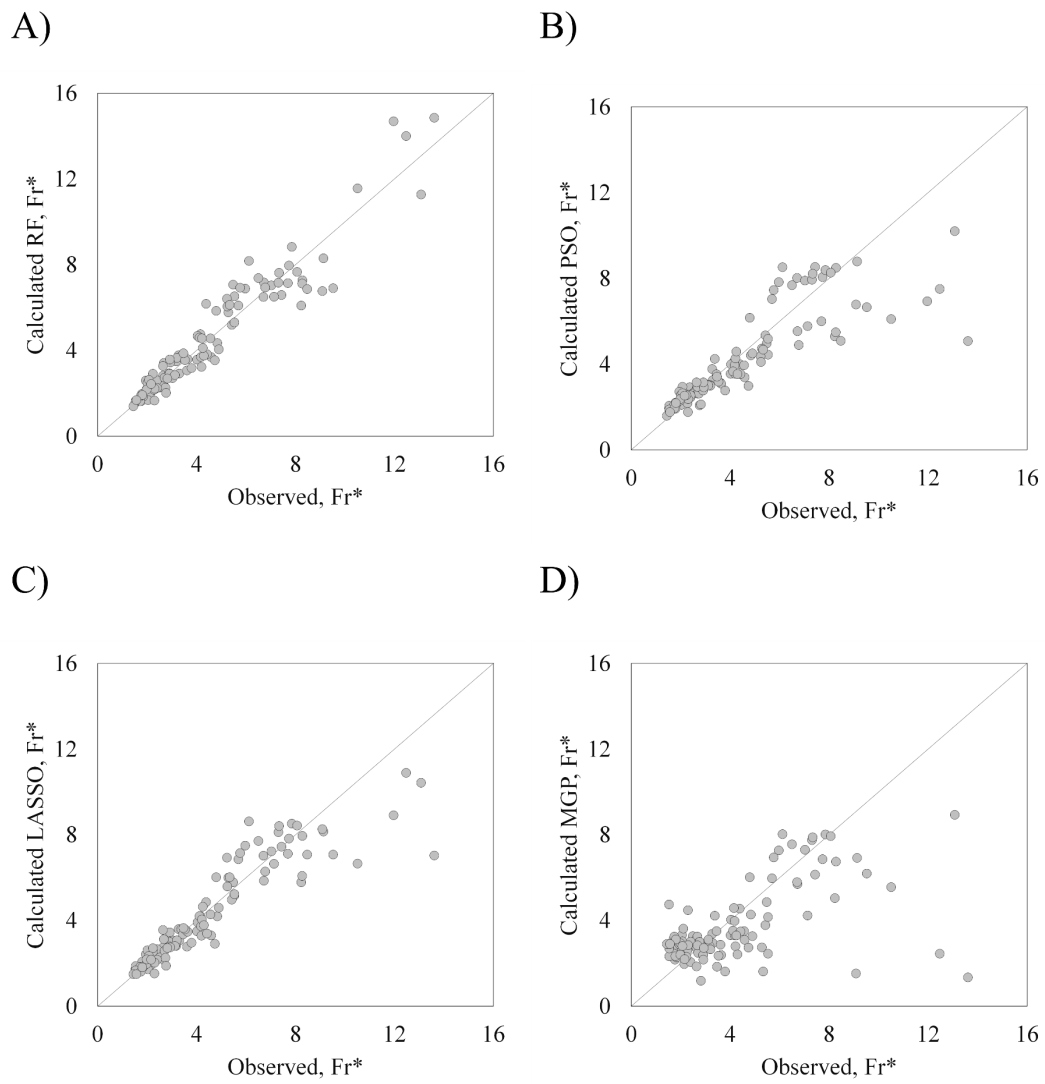
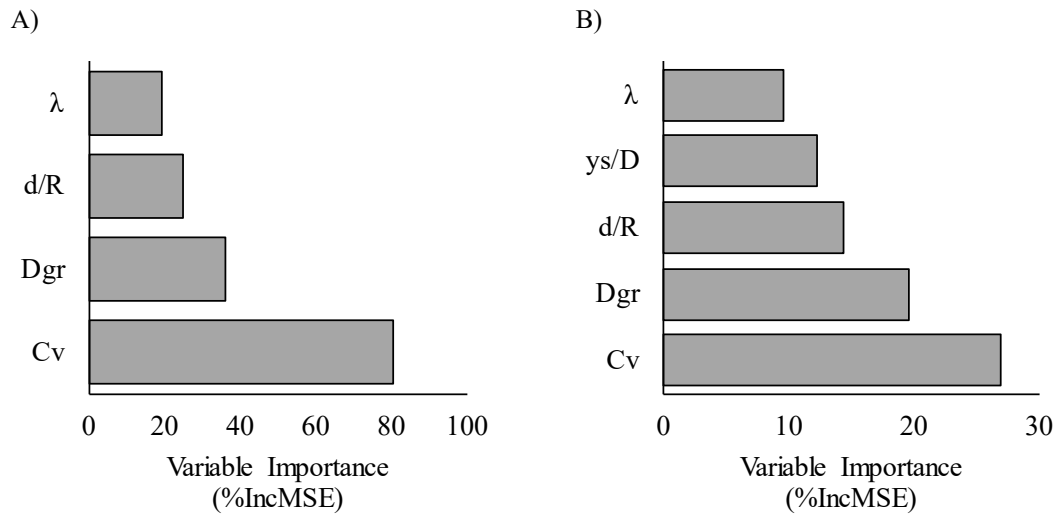


Figure 5. Performance of the models applied in the non-deposition without deposited bed testing dataset.



646  
 647 Figure 6. Performance of the models applied in the non-deposition with deposited bed  
 648 testing dataset.



649

650 Figure 7. Variable importance estimated by RF model: A) without deposited bed; B) with  
 651 deposited bed.